ISSN 0208-7774 TRIBOLOGIA 5/2019 p. 115–124
DOI: 10.5604/01.3001.0013.6568

Sławomir ZIMOWSKI[*], Marcin KOT[*], Grzegorz WIĄZANIA[*], Tomasz MOSKALEWICZ[****]

THE ABILITY OF NANOCOMPOSITE CARBON COATINGS TO WITHSTAND FRICTION UNDER SEVERE CONDITIONS

ZDOLNOŚĆ NANOKOMPOZYTOWYCH POWŁOK WĘGLOWYCH DO TARCIA W EKSTREMALNYCH WARUNKACH

Key words: load carrying capacity, nanocomposite coatings, severe wear.

Abstract The paper presents an analysis of the micromechanical properties of selected thin, hard anti-wear coatings of the type nc-TiN/a-C and nc-TiC/a-C, which were deposited by magnetron sputtering on a steel substrate. The load carrying capacity of the nanocomposite coatings was analysed in point contact with the use of indentation method, a scratch test, and friction test in contact with a ceramic ball. The hardness and modulus of elasticity of the coatings were determined by an instrumented indentation method using a Vickers indenter. The coating adhesion to the substrate was examined in a scratch test. Tribological tests in sliding contact with an Al_2O_3 ball were made at various loads to determine the limit load in which normal friction occurs. The results of tribological tests were compared with the resistance to plastic deformation index (H^3/E^2). It was found that the basic micromechanical parameters of coatings provide important information concerning durability and load carrying capacity. However, while predicting wear, it is also important to investigate the nature of the wear process during friction. The wear nature of the nc-TiN/a-C and nc-TiC/a-C coatings depends on the load value and the number of forced loads.

Słowa kluczowe: nośność, nanokompozytowe powłoki, zużycie patologiczne.

Streszczenie W pracy przedstawiono analizę właściwości mikromechanicznych wybranych cienkich, twardych powłok przeciwzużyciowych typu nc-TiN/a-C oraz nc-TiC/a-C, które zostały osadzone metodą magnetronowego rozpylania na podłożu stalowym. Zdolność nanokopozytowych powłok do przenoszenia obciążeń analizowano w styku skoncentrowanym metodą indentacyjną poprzez testy zarysowania oraz testy tarciowe z ceramiczną kulą. Twardość i moduł sprężystości powłok określono instrumentalną metodą wciskania wgłębnika Vickersa, a adhezję powłok do podłoża zbadano w teście zarysowania. Testy tribologiczne w ślizgowym styku z kulą Al_2O_3 wykonano przy różnych obciążeniach w celu określenia granicznego obciążenia, w którym zachodzi tarcie normalne. Wyniki badań tribologicznych porównano ze wskaźnikiem odporności na plastyczną deformację (H^3/E^2). Stwierdzono, że podstawowe parametry mikromechaniczne powłok niosą ważną informację o trwałości i zdolności do przenoszenia obciążeń, jednak w prognozowaniu zużycia istotne jest również zbadanie charakteru zużycia podczas tarcia. Przebieg procesu zużywania powłok nc-TiN/a-Ci nc-TiC/a-C uzależniony jest od wielkości nacisku oraz liczby wymuszeń obciążeniowych.

INTRODUCTION

Predicting the wear of machine parts, especially kinematic pairs, is important, because it provides an opportunity to increase the durability and reliability of machines and devices. Knowledge of the tribological characteristics of cooperating elements is extremely helpful in this area and gives information about the friction and material wear under certain conditions. Designing a wear-resistant material is possible thanks to knowledge of its

[*] ORCID: 0000-0002-7348-8751. AGH University of Science and Technology, Faculty of Mechanical Engineering and Robotics, A. Mickiewicza 30 Ave., 30-059 Krakow, Poland, e-mail: zimowski@agh.edu.pl.
[**] ORCID: 0000-0002-3017-9481. AGH University of Science and Technology, Faculty of Mechanical Engineering and Robotics, A. Mickiewicza 30 Ave., 30-059 Krakow, Poland.
[***] ORCID: 0000-0001-9247-0015. AGH University of Science and Technology, Faculty of Mechanical Engineering and Robotics, A. Mickiewicza 30 Ave., 30-059 Krakow, Poland.
[****] ORCID: 0000-0001-7142-452X. AGH University of Science and Technology, Faculty of Metals Engineering and Industrial Computer Science, Czarnowiejska 66 Street, 30-059 Krakow, Poland.

mechanical properties and wear in frictional contact. The development of research methods in this field makes it possible to test monolithic materials, coatings, and super thin films under established cooperation conditions **[L. 1, 2]**. On this basis, it is possible to determine the limit external loads of friction pairs that ensure correct cooperation and do not cause severe wear **[L. 3, 4]**. However, external loads should also be understood as various types of external impacts characterizing the environment of the tribological system, e.g., the effect of a chemically aggressive environment **[L. 5]** or friction at elevated temperatures **[L. 6]**. Models for predicting material consumption using basic mechanical parameters are still being developed in order to replace time-consuming and material-consuming tribological experiments. The hardness of the material is often the basic parameter that classifies engineering materials; however, in the case of coatings, this relationship is not always directly proportional. **[L. 7–9]**.

Exceeding the load capacity of the friction pair elements leads to a change in the conditions of cooperation, and thus causes a transition from normal to severe friction (friction where great instability of cooperation is occurred), which is accompanied by severe wear. Pathological forms of abrasive wear include micro-cutting and ploughing **[L. 10]**, and, in the case of coatings their cracking, chipping and delamination **[L. 11, 12]**. In highly loaded kinematic pairs, increased durability is obtained, among others, through the use of hard ceramic **[L. 13]** or carbon coatings **[L. 14, 15]**. Thin anti-wear coatings based on amorphous (a-C) or hydrogenated amorphous carbon (a-C:H) are characterized by great tribological properties; however, brittleness is a big problem in their operation. The brittleness of the coating leads to the formation of microcracks and their propagation, which causes a decrease in the adhesion of the coating to the substrate, chipping of its fragments, and even complete destruction due to delamination. Increasing the load carrying capacity of the coatings and improving their resistance to crack is achieved through creating composite structures by introducing hard nanoparticles into the structure of the coating **[L. 16]**, creating multilayer systems **[L. 17]**, or also doping the carbon coating with other elements, e.g., Ti, W, or Ag **[L. 18]**.

The paper analyses the ability of the coating-substrate system to withstand loading in stationary and sliding point contact under increasing and constant loads.

EXPERIMENTAL

The subject of the study were nanocomposite coatings of the nc-TiN/a-C and nc-TiC/a-C type as well as the unreinforced amorphous carbon a-C coating deposited onto 6 mm thick disc substrates 25.4 mm in diameter made of Vanadis 23 steel. The coatings were produced by magnetron sputtering at the Institute of Materials Science and Engineering of the Lodz University of Technology. The geometrical structure of the sample surface was examined using a Profilm 3D optical profilometer from Filmetrics, USA. Measurements were performed using the contactless method based on the phenomenon of white light interferometry (WLI). Analysis of the obtained 3D surface image by the use of special software for the profilometer allows the determination the surface roughness parameters. The device allows the measurement of roughness parameters with a resolution of 0.1 nm. Profilometric measurements were carried out in order to characterize the geometric structure of the coating's surface and to compare the surface roughness of the coatings and substrate. The results of this research were also helpful in the analysis of coating wear in sliding point contact. Differences in the surface roughness of the tested samples were compared based on the *Ra* and *Sa* parameters determined in accordance with ISO 4287 and ISO 25178, respectively. The *Ra* parameter is referred to as the arithmetic mean roughness value along the sampling length, while *Sa* is the arithmetic mean or average of the absolute distances of the surface points from the mean plane. Four measurements were performed for each sample along the sampling length of 600 μm oriented in different directions (every 45°) as well as on a surface of 500×400 [μm] in accordance with the requirements of ISO standards.

The micro-mechanical property tests of the coatings, including the indentation tests using a Vickers indenter and scratch tests using a Rockwell C indenter with a tip radius of 0.2 mm, were performed with a Micro-Combi-Tester (MCT) from CSM Instruments. The hardness and elastic modulus of the coatings were determined by the instrumental indentation method using the commonly known Oliver and Pharr model **[L. 19]**. The indentation measurements were repeated ten times at the same load of 10 mN, with a new area of the sample used each time. The crack resistance of coatings and load carrying ability of the coating/substrate system in point contact was also investigated in indentation tests under the many times higher load of 10000 mN.

The adhesion of the coating to the substrate was examined by a standardized scratch method in accordance with the PN-EN ISO 20502:2016 standard. The tests were carried out using the Micro-Combi-Tester device, in which the maximum load of indenter is 30 N. The degree of the coating adhesion to the substrate is described by the critical load, i.e. the indenter load that causes the characteristic form of the coating failure. Three tests were performed for each coating using a Rockwell C diamond indenter with the following parameters: a scratch length of 5 mm, a progressive load in the range of 0.01–30 N, and the relative speed of the indenter was 5 mm/min.

Tribological tests were performed in non-lubricated sliding contact with a ball of 1 mm in diameter made of aluminium oxide (Al_2O_3) with a hardness of 19 GPa. Tests were carried out at the loads of 1, 2, 4, 8, and 10 [N]

with a set average sliding speed of 0.05 m/s on a 500 m sliding distance, which corresponded to 20000 cycles. Before each test, the surfaces of the balls and coatings were washed with an alcohol solution and allowed to dry. Three repetitions for each friction pair and each load were performed. The wear rate W_v of the coating [mm^3/Nm] was determined according to Equation (1):

$$W_v = \frac{V_{coating}}{L \cdot s} \quad (1)$$

where $V_{coating}$ is the wear volume of the coating calculated from the cross-sectional area of the wear track measured by a contact stylus profilometer (mm^3), L is the applied normal load (N), and s is the sliding distance (m).

The analysis of the coating wear mechanism was based on observations of the coating wear tracks and scars on the balls using a light microscope (LM) provided with the MCT device. The LM microscope has an optical system composed of three Nikon 5x/0.13, 20x/0.46, and 50x/0.80 lenses as well as a PULNiX digital camera with 10x magnification eyepiece.

RESULTS AND DISCUSSION

Material characterization

The a-C carbon coating and nanocomposite nc-TiN/a-C and nc-TiC/a-C coatings produced by magnetron sputtering were investigated. As previous microstructure studies have shown **[L. 20]**, the composite coatings consisted of an amorphous carbon matrix and evenly distributed particles of nc-TiN or nc-TiC nanocrystallites formed during the process of magnetron sputtering. The average content of nanocrystallites did not exceed 10 vol. %, and their diameter was 2–3 nm and 5 nm for nc-TiC and nc-TiN, respectively **[L. 20]**. The coatings were deposited on model Vanadis 23 sintered high speed steel (weight % composition: 1.28 C, 4.2 Cr, 5 Mo, 6.4 W, 3.1 V), which was manufactured by Uddeholm, Sweden. Vanadis 23 steel substrates were heat treated by quenching at 1150°C and tempering twice at 550°C for 1 hour. After hardening, the surfaces of the steel substrates were polished, reaching an average roughness value of Ra = 0.02 µm, measured in different directions. In the first stage, a very thin interlayer of pure titanium with a thickness of ~ 20 nm was applied to the polished substrates. Next, the amorphous carbon a-C and nanocomposite nc-TiN / a-C and nc-TiC / a-C coatings with a thickness of about 2 µm were deposited.

The a-C coating shows considerably more surface defects in the form of micro-crates, and its surface roughness determined by the parameter Ra = 0.0037 ±0.0011 µm was the highest (Sa = = 0.0237 µm). The nanocomposite coatings were uniform without discontinuities as well as being smoother. The surface roughness of the nc-TiN/a-C and nc-TiC/a-C coatings was comparable and reached the value of Ra = 0.0031 ±0.0009 µm and Ra = 0.0027 ±0.0002 µm, respectively (and Sa = 0.0058 µm and Sa = 0.0045 µm, respectively). The surfaces of the deposited coatings were characterized by roughness parameters an order of magnitude smaller than the steel substrate. The surface state of the coatings is shown in **Fig. 1.**

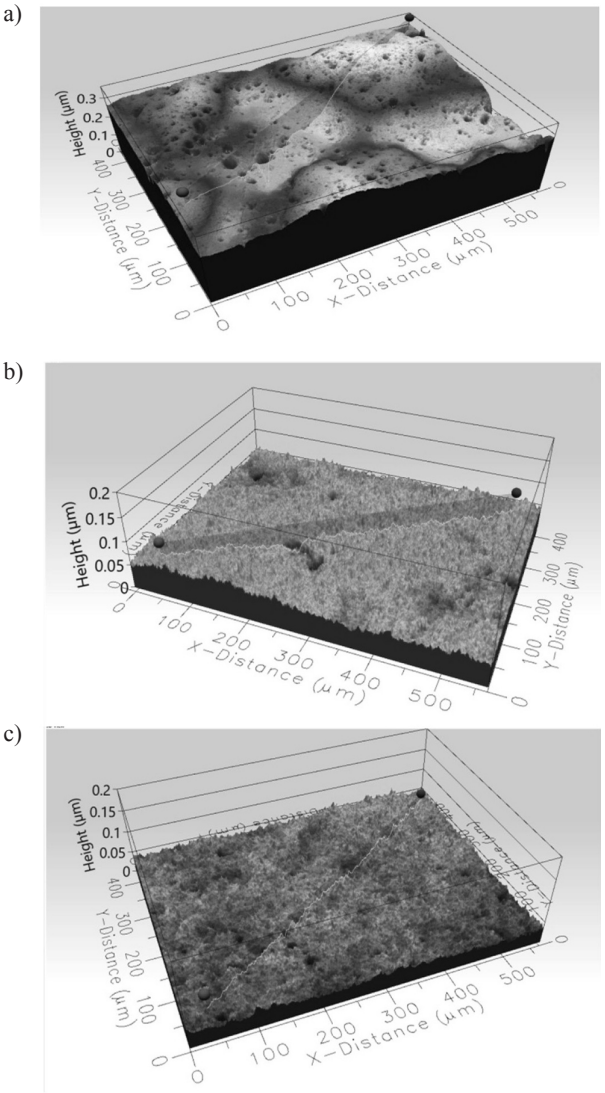

Fig. 1. Surface image of the a-C (a), nc-TiN/a-C (b) and nc-TiC/a-C (c) coatings deposited on Vanadis 23 steel

Rys. 1. Obraz powierzchni powłok: a-C (a), nc-TiN/a-C (b) oraz nc-TiC/a-C (c) osadzonych na stali Vanadis 23

Indentation resistance of the coatings

The hardness (H) and elastic modulus (E) of the anti-wear coatings are the basic mechanical properties that are used in modelling of their resistance to abrasion. The load carrying ability of the coatings in concentrated contact is related to their hardness, i.e. the resistance of the coating to localized pressing of the indenter. For a sharp

indenter, plastic deformation starts in the coating at very low loads. The zone of the plastic deformation under the indenter most often has the shape of a hemisphere, and the volume of the plastic zone increases as the load increases. This zone will grow until its radius is equal to the coating thickness before the substrate beneath it starts to plastically deform **[L. 8]**. It is often observed that the volume of the deformed material under the indenter is approximately hemispherical. In studies of monolithic materials, tested with the Vickers indenter, it was shown that the radius of the plasticized zone R_{pl} can be defined by the following equation **[L. 21]**:

$$R_{pl} = k_2 \delta \left(\frac{E}{H} \right)^{1/2} cot^{1/3} \psi \qquad (2)$$

where k_2 – a specific constant typical for the indenter geometry ($k_2 = 3.5$ for the Vickers indenter), δ – indentation depth, E – Young's modulus, and H – hardness, $\psi = 0.71$ – the effective indenter angle (it is usual to use the angle of a cone which displaces an equivalent amount of material as a faceted indenter).

In indentation measurements, where the H and E of thin coatings are determined, the relation of the penetration depth of the indenter to the coating thickness is very important. Exceeding the limit value of the penetration depth means the substrate properties affect the measured parameters. The value of indentation depth is related to the radius of the plastic zone of the coating and can be estimated according to Equation (2) if the indenter geometry and indentation depth are known. If we equate the indentation depth to the coating thickness (t) and rearrange equation (2), we obtain the following:

$$\frac{\delta}{t} = 0.4 \left(\frac{H}{E} \right)^{1/2} \qquad (3)$$

For typical hard coatings, such as TiN, the H/E ratio reaches the value 0.1; hence, the penetration depth of the indenter is 0.126 t (approximately $t/10$) before the critical plastic deformation of the substrate is achieved. If we test soft coatings, the H/E ratio decreases, and the critical value of δ/t decreases below 10%. The assumption $\delta = t/10$ is not valid if the substrate is harder than the coating, and it may not plastically deform in these circumstances **[L. 8]**.

In the presented investigations, the hardness measurements were performed at a load of 10 mN, which corresponded to the average penetration depth of the indenter equal 150 nm and 164 nm for the nc-TiN/a-C and nc-TiC/a-C coatings, respectively. According to the methodology of hardness measurement of thin coatings, an indentation depth of the indenter below 0.1 of the coating thickness ensures the properties of the coating material are obtained without affecting the properties of the substrate. The load carrying capacity of the coatings is also described by the relation of their hardness and modulus of elasticity. The H/E ratio, called the *plasticity index*, is related to the elastic deformation to the destruction of the coating, while the H^3/E^2 *index* describes the resistance to plastic deformation. The increase in the value of these indicators leads to an improvement in the load carrying capacity of the coating-substrate system. The determined values of the hardness and elastic modulus as well as the H/E and H^3/E^2 indicators are given in **Table 1**.

The introduction of nanoparticles reduced the hardness of nanocomposite coatings compared to the a-C matrix. However, a definite benefit was the increase in their fracture toughness, which was confirmed in high load indentation tests. In order to induce a sufficient concentration of high stresses in the coating, a sharp Vickers indenter was used, which was pressed with a 10000 mN load. The dependence of the indenter displacement and load for typical measurements at high load is shown in **Fig. 2**.

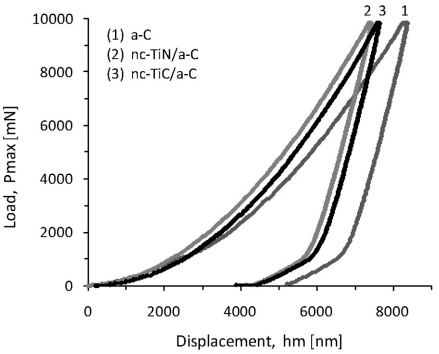

Fig. 2. Plot of a load-displacement curve obtained from indentation of the a-C, nc-TiC/a-C and nc-TiN/a-C coatings on Vanadis 23 steel

Rys. 2. Krzywa obciążenie-przemieszczenie podczas indentacji powłok a-C, nc-TiC/a-C oraz nc-TiN/a-C osadzonych na stali Vanadis 23

Table 1. Hardness H and elastic modulus E at the load of the indenter 10 mN
Tabela 1. Twardość H i moduł sprężystości E przy obciążeniu wgłębnika 10 mN

Sample	t [μm]	h_{max} [nm]	H [GPa]	E [GPa]	H/E	H^3/E^2 [GPa]
a-C on Vanadis 23	1.8	125 ±2	17.8 ±1.9	183 ±11	0.096	0.168
nc-TiN/a-C on Vanadis 23	2.1	150 ±10	16.1 ±1.0	189 ±8	0.085	0.115
nc-TiC/a-C on Vanadis 23	1.9	164 ±8	13.9 ±1.3	178 ±9	0.079	0.085
Vanadis 23	---	245 ±11	10.5 ±0.9	221 ±6	---	---

The Vickers tests performed with 100 times higher load than during hardness measurements of the coatings showed large cracks of the carbon coating (a-C), which at the beginning propagated from the corners of the imprint and, as a consequence, caused chipping of the coating **(Fig. 3a)**. These investigations confirmed a significantly lower ability to take high loads in the concentrated contact by the a-C coating compared to the nanocomposite nc-TiN/a-C and nc-TiC/a-C coatings. The greater brittleness of the a-C coating in point contact was due to its surface defects and greater roughness compared to the others coatings. Both nanocomposite coatings under the same conditions of high stress concentration only underwent plastic deformation without cracks and chipping of their fragments **(Figs. 3b, c)**.

The penetration depth at a load of 10000 mN reached a value up to 8 μm and was, on average, four times greater than the thickness of the coating. One negative effect of coating cracking is a decrease in the corrosion resistance of the coating-substrate system, due to the break in the continuity of the coating structure, which occurs even in stationary contact. However, during operation, e.g., in frictional contact, cracks can propagate and lead to the separation of the coating from the substrate and lower load capacity of the friction pair. In addition, the separated hard coating particles present in the friction zone will accelerate wear **[L. 22]**. Contact with the wear particles will additionally increase the stress concentration in the micro-areas.

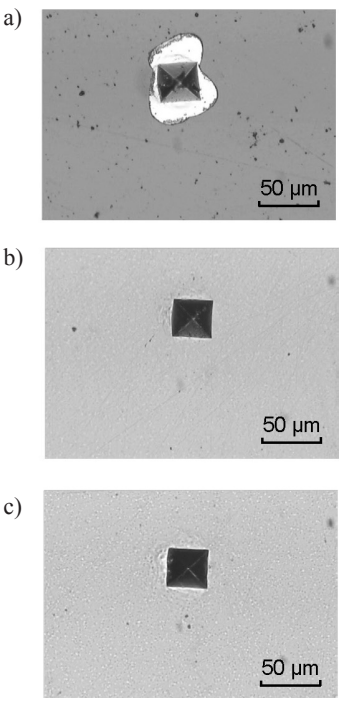

Fig. 3. Imprints of the coatings: a) a-C, b) nc-TiC/a-C, c) nc-TiN/a-C on Vanadis 23 steel after indentation at 10000 mN, (LM, mag. 200x)

Rys. 3. Obrazy odcisków po wciskaniu wgłębnika z obciążeniem 10000 mN powłok: a) a-C, b) nc-TiC/a-C, c) nc-TiN/a-C na stali Vanadis 23, (LM, pow.200x)

Scratch resistance of the coatings

The adhesion of the coating to the substrate is the main parameter that determines the capability of using the coating-substrate system. The scratch test is a common, standardized method for testing the adhesion of a coating to a substrate. In this test, spherical indenters as scratch probes are pressed against the moving coating with progressive load and scratch its surface. Analysis of the scratch track and the measured parameters, such as friction force, geometry of the scratch track and acoustic emission, allow the scratch resistance of the coating to be determined. The critical load (L_C) causing the characteristic form of coating damage is a measure of the degree of coating adhesion to the substrate. The load causing cohesive cracks is determined by L_{C1}. The L_{C2} critical load initiates adhesive type cracks (e.g., coating chipping) or destruction leading to exposed substrates (e.g., coating abrasion). The load causing the complete delamination of large areas of the coating is named L_{C3}. The scratch test may also reflect the behaviour of the coating-substrate system in highly loaded point sliding contact. During the test, a standard Rockwell C indenter with a radius of 0.2 mm at a 30 N load exerts the average contact pressure of several GPa. Such a load occurs during the operation of anti-wear coatings in highly loaded friction nodes, e.g., in the contact of a cutting edge tool **[L. 23]**.

In the heavy concentrated contact during the indenter movement in scratch tests, both composite nc-TiN/a-C and nc-TiC/a-C coatings, showed excellent scratch resistance **(Figs. 4a, b)**. In the scratch tracks of these coatings, no damage of an adhesive type was observed under the load range up to 30 N (maximally load in MCT). A few cohesive cracks occurred only in the nc-TiN/a-C coating at a 28 N load, and this load was taken as L_{C1}. In contrast, the unreinforced a-C coating exhibited significantly less scratch resistance and less ability to carry such heavy loads as nanocomposite coatings. Adhesive cracks result in spallation of large fragments of the a-C coating were found at L_{C2} = 12 N **(Fig. 4 c)**.

In order to determine the coating strength and better characterize the load capacity of the coating-substrate system, the contact pressures that occurred during scratching, $p_{m(Sc)}$, were calculated. The method described by Beake et al. **[L. 24]** enables the yield stresses and the pressure required for the coating failure to be estimated from contact mechanics, assuming the geometry of a scratch track is known and provided that spherical indenters are used. Using spherical probes, the contact depth h_p and the contact radius a in scratch contact can be calculated from the following relationships **[L. 24]**:

$$h_p = \frac{\left(P_d + R_d\right)}{2} \tag{4}$$

and

$$a = \sqrt{2Rh_p - h_p^2} \tag{5}$$

where h_p – the contact depth, P_d – the on-load L scratch depth, R_d – the residual depth from the final scan of the scratch track, a – the contact radius, and R – the radius of the tip indenter.

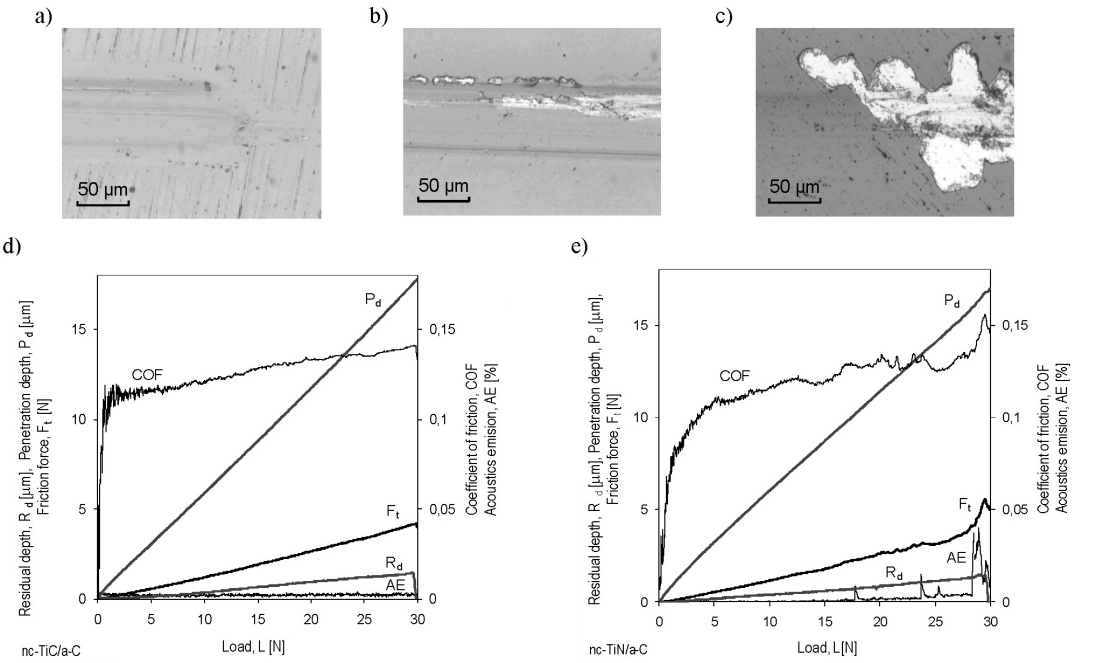

Fig. 4. Scratch track images of the coatings a) nc-TiC/a-C at 30 N, b) nc-TiN/a-C at L_{C1}=28 N, c) a-C at L_{C2}=12 N, (LM, mag. 200x) and scratch results of the d) nc-TiC/a-C coating, e) nc-TiN/a-C coating

Rys. 4. Obrazy toru zarysowania powłok a) nc-TiC/a-C przy 30 N, b) nc-TiN/a-C przy L_{C1}=28 N, c) a-C przy L_{C2}=12 N, (LM, mag. 200x) oraz wyniki testów zarysowania dla powłok d) nc-TiC/a-C, e) nc-TiN/a-C

The mean contact pressure $p_{m(Sc)}$ at any point along the scratch track at load L is calculated according to the following equation:

$$p_{m(Sc)} = \frac{L}{\pi a^2} \tag{6}$$

The contact pressure distribution in the scratch test depends on the rate of change in the indenter's contact area with the coating **(Fig. 5)**. In the initial period, when the contact area is very small, the contact pressure $p_{m(Sc)}$ increases rapidly until the steady state is reached. Due to the comparable mechanical properties of the tested coatings, the differences in the values of contact pressures are not large and equal 2.55 GPa and 2.67 GPa for nc-TiC/a-C and nc-TiN/a-C, respectively. The nc-TiC/a-C coating is more susceptible to deformation; therefore, its contact area is higher compared to nc-TiN/a-C. Therefore, in contact with the Rockwell indenter, the heavy contact pressure is released but is perfectly absorbed by both composite coatings. The coatings able to carrying such heavy loads in point contact will also work well in area contact, e.g., as coatings for plain bearings.

The most intense conditions of cooperation occur in those kinematic pairs that work in point contact. Therefore, the results of scratch tests carry much information about the ability to carry loads through hard coatings. This method works well in assessing the scratch resistance as well as the interface strength of coatings in sliding contact at both low and high loads. In addition, scratch tests at progressive loads make it possible to assess the load carrying capacity of a coating/substrate system over the entire load range in one test **[L. 24]**.

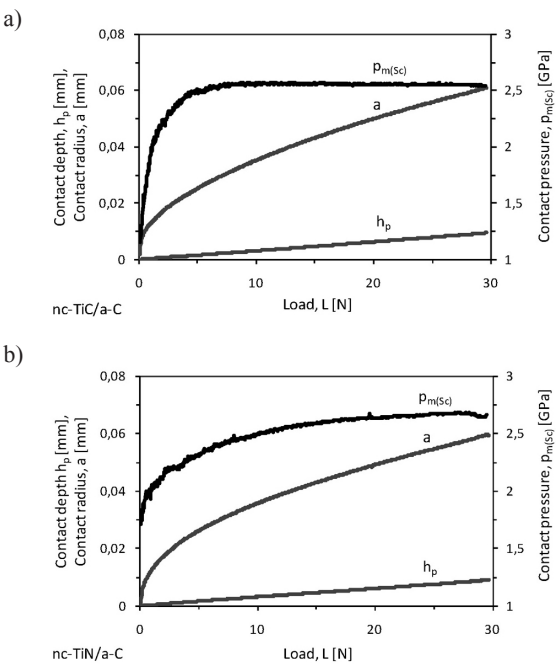

Fig. 5. Contact pressure at successive points along the scratch track of the a) nc-TiC/a-C and b) nc-TiN/a-C coating

Rys. 5. Rozkład nacisków stykowych w kolejnych punktach wzdłuż toru zarysowania dla powłoka) nc-TiC/a-C oraz b) nc-TiN/a-C

Wear resistance of the coatings

Despite the many metrological advantages of the scratch test, it does not fully reflect the frictional behaviour of the tested materials. The reason for this is the application of a load that often leads to plastic deformation as well as a one-time contact of the probe with the tested element along the scratch track. During operation of the kinematic pairs in concentrated sliding or rolling contact, the external interactions are cyclical. In sliding contact, the tribological wear is further enhanced by fatigue effects. The ball sliding on the surface of the coating at a given moment is in contact with the coating at one point. There is compressive stress in front of the counter-element and tensile stress behind the contact zone, and their values are very high due to the stress concentration. These conditions cause continuous deformation of the coating-substrate system at a frequency connected with rotational speed and friction radius.

The value of the deformation is closely related to the load, which in the tested friction contact with an Al_2O_3 ball of 1mm in diameter at the initial time caused the average contact pressure of 3.5 GPa (at a 10 N load). Therefore, the nature of the wear of the nc-TiN/a-C and nc-TiC/a-C coatings depends on the value of these pressures and the number of load impacts **(Fig. 6)**. The a-C coating was not considered in tribological investigation due to its much lower scratch resistance and brittleness compared to nanocomposite coatings. At a low load of 1–5 N (pm = 1.6–2.8 GPa), the wear of both composite coatings was mainly abrasive. In the wear tracks, neither coating cracks nor any significant plastic deformation of the coating-substrate system were observed, mainly due to the high rigidity of the steel substrate, which provided good support for the coating. However, at 8 N (pm = 3.3 GPa), local failure in the form of cracks and chipping of the nc-TiN/a-C coating was found **(Figs. 6c, d)**. This behaviour was caused by the higher surface roughness of this coating and its poorer local quality due to material defects in form of microcracks or voids.

The highest wear resistance was found for the nc-TiC/a-C coating, despite its smaller hardness and H^3/E^2 ratio compared to the nc-TiN/a-C coating **(Table 2, Fig. 7)**. The wear index determined at a load of 1 N equalled 0.07 * 10^{-6} mm^3/Nm for the nc-TiC/a-C

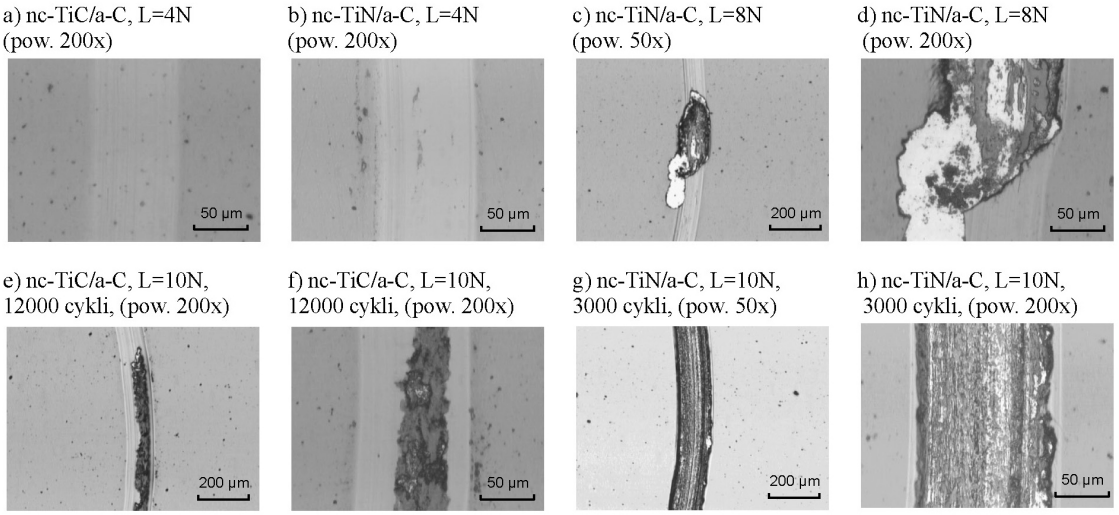

Fig. 6. Micrographs of the wear track of the nc-TiC/a-C and nc-TiN/a-C coatings after friction with Al_2O_3 ball at different load (LM, mag. 50x and 200x)

Rys. 6. Obrazy torów zużycia powłok nc-TiC/a-C oraz nc-TiN/a-C po tarciu z kulą Al_2O_3 przy różnych obciążeniach, (LM, pow. 50x i 200x)

Table 2. Wear rate (W_v) and friction coefficient (COF) of the nc-TiC/a-C and nc-TiN/a-C coatings, *) COF at the time when the coating was failure to the substrate

Tabela 2. Wskaźnik zużycia objętościowego (W_v) oraz średni współczynnik tarcia (COF) powłok nc-TiC/a-C oraz nc-TiN/a-C, *) COF w okresie kiedy powłoka została zniszczona do podłoża

Coating	Parameter	Load, L [N]				
		1	2	4	8	10
nc-TiC/a-C	$W_v \cdot 10^{-6}$ [mm^3/Nm]	0.07 ±0.01	0.06 ±0.01	0.26 ±0.03	0.3 ±0.06	0.84 ±0.09
	COF (mean)	0.05	0.06	0.06	0.08	0.12 / 0.55*
nc-TiN/a-C	$W_v \cdot 10^{-6}$ [mm^3/Nm]	0.13 ±0.03	0.14 ±0.03	0.33 ±0.02	0.50 ±0.08	1.24 ±0.08
	COF (mean)	0.07	0.07	0.12	0.13	0.15 / 0.60*

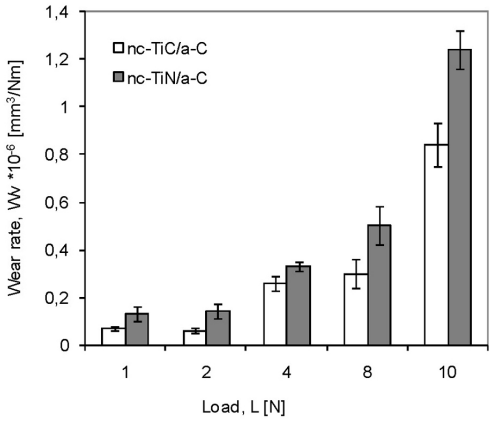

Fig. 7. Wear rate of the nc-TiC/a-C and nc-TiN/a-C coatings
Rys. 7. Wskaźnik zużycia objętościowego powłok nc-TiC/a-C oraz nc-TiN/a-C

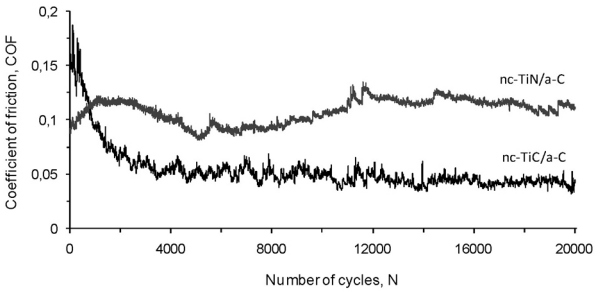

Fig. 9. Friction coefficient of the coatings in dry sliding contact against Al_2O_3 ball under load of 4 N
Rys. 9. Współczynnik tarcia powłok w styku ślizgowym z kulą Al_2O_3 przy obciążeniu 4 N

coating and was nearly twice as low as the wear rate for the nc-TiN/a-C coating. Such good wear resistance of the nc-TiC/a-C coating results from the creation of a self-lubricating sliding film in the friction process, which significantly reduces the resistance to movement and contributes to less abrasive wear of the coating **(Fig. 8)**.

This is confirmed by the coefficient of friction with a value, at the lowest load, of only 0.05 **(Fig. 9)**. The characteristic behaviour during friction of carbon coatings is the occurrence of the graphitization process and formation of a self-lubricating film **[L. 25]**. This graphite-like film separates the contact between the cooperating elements, and the ball slides more easily against the counter-element and results in less abrasive wear of the coating. However, the presence of hard nanoparticles in sliding contact may limit the ability to form a self-lubricating film on the friction surface. This effect can be seen in the case of friction of the nc-TiN/a-C coating, where a mild reduction in the friction coefficient was not observed.

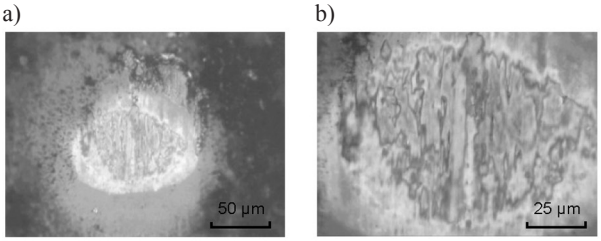

Fig. 8. Image of the self-lubricated layer formed on the Al_2O_3 ball during friction with nc-TiC/a-C coating, (LM, pow. 200x (a), 500x (b))
Rys. 8. Obraz powierzchni kuli Al_2O_3 z widoczną warstwą samosmarną powstałą podczas tarcia z powłoką nc-TiC/a-C, (LM, pow. 200x (a), 500x (b))

At the load of 8 N, the wear intensity of the coatings increased significantly **(Fig. 7)**. The higher wear of the coatings was caused by the more rugged conditions of cooperation due to the increase in contact pressure and as well the presence of hard wear products in the friction zone, mainly consisting of the coating material. However, under these conditions ($p_{m\,(8N)}$ = 3.3 GPa), both nano-coated coatings transferred the given load within a specified time and were not subjected to sharp wear. However, with a load of 10 N ($p_{m\,(10N)}$ = 3.5 GPa), severe wear of the nc-TiN/a-C coating was found above 2500 cycles, and severe wear of the nc-TiC/a-C coating was found after about 12000 cycles. The process of coating destruction took place gradually, but more rapidly in the case of the coating strengthened with TiN nanoparticles. At first, cracks appeared in the coating, then the spalling of the coating occurred and the hard wear products present in the friction track accelerated grinding and abrasion, which intensified the wear process. Observations of the coating wear tracks after friction at 10 N were possible because the tests were broke when the measured friction force increased significantly. The results obtained in this way were used to determine the wear indexes refer mainly to the coating material.

SUMMARY

The investigations have confirmed that increasing the load carrying capacity of amorphous carbon coatings and thus improving their wear resistance can be achieved by composite structures created by the incorporation of hard nanoparticles into the coating structure. Titanium carbides (TiC) and titanium nitrides (TiN) formed during the deposition process enhanced the properties of the a-C coatings and increased the durability of composite coatings based on this amorphous carbon. The a-C coating showed a significantly lower ability to bear high contact pressure compared to the nc-TiN/a-C and nc-TiC/a-C nanocomposite coatings. In both nanocomposite coatings under the same conditions at high stress concentrations, only plastic deformation

occurred without cracks or chipping. These composite coatings also exhibited very good scratch resistance, which guarantees their good adhesion to the substrate. In contact with the Rockwell indenter, very high contact stresses (up to 2.7 GPa) were released, which were perfectly absorbed by both composite coatings. The distribution of contact pressure in the scratch test depends on the rate of the contact area changes. A full picture of the behaviour of hard anti-wear coatings was obtained on the basis of friction tests. In the sliding point contact, the wear of the coatings was mainly abrasive and was further intensified by the local fatigue effects.

The value of deformation of the coating/substrate system is closely related to the load, which, in the tested friction contact with a 1mm of diameter alumina ball, caused the average initial contact pressure of even 3.5 GPa. Therefore, the nature of the wear of the nc-TiN/a-C and nc-TiC/a-C coatings depended on the value of these pressures and the load cyclicity in sliding point contact. At higher contact pressures, above pm = 3.3 N, the wear intensity of the coatings increased significantly. The sliding friction coefficient of the nc-TiC/a-C coating equal to 0.05 was the smallest. Very good sliding properties of the nanocomposite carbon coatings are ensured by creating a self-lubricating film in frictional contact. However, the presence of hard nanoparticles in sliding contact may limit the formation of this self-lubricating film.

ACKNOWLEDGEMENTS

This work was supported by the Polish Ministry of Science and Higher Education under subvention funds for the Department of Machine Design and Exploitation of AGH-UST (AGH grant number 16.16.130.942).

REFERENCES

1. Stachowiak G.W., Batchelor A. W., Stachowiak G.B.: Experimental methods in tribology. In Tribology series vol. 44, Chapter 2 and 3. Elsevier 2004.
2. Giannakopoulos A.E., Suresh S.: Determination of elastoplastic properties by instrumented sharp indentation. Scripta Materialia 40 (1999), pp. 1191–1198.
3. Ghaderi A., Saha G., Guo T., Fabijanic D., Barnett M.R.: Material wear map for ground-engaging steels based on scratch tests. Wear 404 (2018), pp. 153–165.
4. Chronowska-Przywara K., Kot M.: Wpływ parametrów badań na deformację i pękanie układu powłoka-podłoże w wyniku próby zarysowania. Tribologia 2 (2014), pp. 19–29.
5. Marciano F.R., Costa R.P.C., Lima-Oliveira D.A., Lobo A.O., Corat E.J., Trava-Airoldi V.J.: Tribological behavior under aggressive environment of diamond-like carbon films with incorporated nanocrystalline diamond particles. Surface and Coatings Technology 206 (2011), pp. 434–439.
6. Zimowski S.: Self-lubricating properties of thin coatings based on molybdenum disulphide. Tribologia 3 (2016), pp. 205–215.
7. Kot M., Rakowski W., Lackner J.M., Major Ł.: Analysis of spherical indentations of coating-substrate systems: experiments and finite element modeling. Materials and Design 43 (2013), pp. 99–111.
8. Bull S.J.: Nanoindentation of coatings. Journal of Physics D: Applied Physics 38(24), (2005) R393-R413.
9. Zimowski S.: Wpływ twardości i modułu sprężystości powłok kompozytowych na ich odporność na zużycie. Tribologia 4 (2014), pp. 149–160.
10. Kato K.: Classification of wear mechanisms/models. Proceedings of the Institution of Mechanical Engineers, Part J: Journal of Engineering Tribology 216 (2002), pp. 349–355.
11. Holmberg K., Ronkainen H., Matthews A.: Wear mechanisms of coated sliding surfaces. In Tribology series vol. 25. Elsevier 1993, pp. 399–407.
12. Piekoszewski W., Szczerek M.: Mechanizmy niszczenia warstw powierzchniowych elementów z powłokami PVD przez pitting. Tribologia 4 (2011), pp. 229–243.
13. Hogmark S., Jacobson S., Larsson M.: Design and evaluation of tribological coatings. Wear 246 (1–2), (2000), pp. 20–33.
14. Michalczewski R., Piekoszewski W.: Wear and friction characteristics of low friction coatings in dry conditions. Tribologia 26 (2007), pp. 9–21.
15. Madej M.: The effect of TiN and CrN interlayers on the tribological behavior of DLC coatings. Wear, 317(2014), pp. 179–187.
16. Zimowski S., Kot M., Moskalewicz T.: The Effect of MeC Nanoparticles on the Micromechanical and Tribological Properties of Carbon Composite Coatings. Tribologia 4 (2018), pp. 157–163.
17. Sui X., Liu J., Zhang S., Yang J., Hao J.: Microstructure, mechanical and tribological characterization of CrN/DLC/Cr-DLC multilayer coating with improved adhesive wear resistance. Applied Surface Science 439 (2018), pp. 24–32.

18. Qiang L., Zhang B., Zhou Y., Zhang J.: Improving the internal stress and wear resistance of DLC film by low content Ti doping. Solid State Sciences 20 (2013), pp. 17–22.
19. Pharr G. M., Oliver W. C.: Measurement of thin film mechanical properties using nanoindentation. Mrs Bulletin 17 (1992), pp. 28–33.
20. Moskalewicz T., Wendler B., Czyrska-Filemonowicz A.: Microstructural characterisation of nanocomposite nc-MeC/aC coatings on oxygen hardened Ti-6Al-4V alloy. Materials Characterization, 61 (2010), pp. 959–968.
21. Lawn B. R., Evans A.G., Marshall D.B.: Elastic/plastic indentation damage in ceramics: the median/radial crack system. Journal of the American Ceramic Society 63 (1980), pp. 574–581.
22. Matthews A., Franklin S., Holmberg K.: Tribological coatings: contact mechanisms and selection. Journal of Physics D: Applied Physics 40 (2007), pp. 5463–5475.
23. Woon K.S., Rahman M., Neo K.S., Liu K.: The effect of tool edge radius on the contact phenomenon of tool-based micromachining. International Journal of Machine Tools and Manufacture, 48 (2008), pp. 1395–1407.
24. Beake B.D., Harris A.J., Liskiewicz T.W.: Review of recent progress in nanoscratch testing. Tribology-Materials, Surfaces & Interfaces 7(2) (2013), pp. 87–96.
25. El Mrabet S., Abad M.D., Sánchez-López J.C.: Identification of the wear mechanism on WC/C nanostructured coatings. Surface and Coatings Technology 206 (2011), pp. 1913–1920.